Metabolomic Profiling on Plasma Reveals Potential Biomarkers for Screening and Early Diagnosis of Intestinal-type Gastric Cancer and Precancerous Stages

Lijing Du[1,2,#], Shasha Li[2,#], Xue Xiao[3], Jin Li[4], Shuai Ji[6], Wenlu Chen[2], Huizi Jin[1], Zhaolai Hua[5], Juming Ma[4], Xi Wang[4,*], Shikai Yan[1,*]

1. School of Pharmacy, Shanghai Jiao Tong University, Shanghai 200240.
2. The Second Clinical College of Guangzhou University of Chinese Medicine, Guangzhou, Guangdong 510006.
3. Institute of Traditional Chinese Medicine, Guangdong Pharmaceutical University, Guangzhou, Guangdong 510006.
4. Department of Oncology, The 903rd Hospital of PLA, Hangzhou, Zhejiang 310013.
5. People's Hospital of Yangzhong City, Yangzhong, Jiangsu 212200, P.R. China.
6. School of Traditional Chinese Medicine, Southern Medical University, Guangdong, Guangzhou 510515, China.

# Lijing Du and Shasha Li contributed equally to the manuscript

*Corresponding authors: Shikai Yan, E-mail: shkyan@sjtu.edu.cn; Xi Wang, E-mail: d.wangxi@hotmail.com.

Abstract

Background: Gastric cancer (GC) faces a great challenge in the clinical diagnosis, that it often can be detected at advanced stages, and leads to the loss of optimum time for treatment and poor prognosis. Thus, there is a critical need to develop effective and noninvasive strategies for early diagnosis of the disease process.

Methods: Totally, 82 participants were enrolled in the study, including 50 chronic superficial gastritis (CSG) patients, 7 intestinal-type early gastric cancer (EGC) and 25 intestinal-type advanced gastric cancer (AGC) ones. Metabolites profiling on patient plasma was performed using ultra-high performance liquid chromatography coupled with quadrupole-time-of-flight mass spectrometry. Orthogonal partial least squares-discriminant analysis was utilized to evaluate the variation on endogenous metabolites for intestinal-type GC patients and to screen potential biomarkers. Furthermore, the proposed biomarkers were used to create random forest models, which discrimination efficiency and accuracy was ascertained by receiver operating characteristic curve (ROC) analysis.

Results: There were eight differential metabolites between the CSG and GC groups, of which four metabolites were increased and four were decreased. L-carnitine, L-proline, pyruvaldehyde, phosphatidylcholines (PC) (14:0/18:0), lysophosphatidylcholine (14:0) (LysoPC 14:0), lysinoalanine were defined as the potential biomarker panel for the diagnosis among CSG and EGC patients. Compared with EGC patients, 6 significantly changed metabolites, PC(O-18:0/0:0) and LysoPC(20:4(5Z,8Z,11Z,14Z)) were found to be up-regulated in AGC patients,

whereas L-proline, L-valine, adrenic acid and pyruvaldehyde down-regulated. The metabolomic pathway analysis revealed several metabolism pathway disorders, mainly involved in amino acid and lipid metabolisms and glycolysis patients. ROC analysis demonstrated a high diagnostic performance in disease diagnosis between CSG and GC.

Conclusion: The result indicated that the biomarker panels are sensitive to the early diagnosis of intestinal-type GC disease, which is expected to be developed as a promising diagnostic and prognostic tool for disease stratification studies.

Key words**:** Intestinal-type gastric cancer, Metabolomics, Biomarkers, Pathway analysis, Random Forest model, UPLC-Q-TOF/MS

Introduction

The International Agency for Research on Cancer estimates that gastric cancer (GC) is the fifth most prevalent malignancy and the third mortality of cancer death all over the world [1]. GC presents in two major distinct morphological subtypes, intestinal and diffuse-type gastric cancers. The intestinal-type GC predominates in high risk geographic areas, such as China, and its incidence increases with age. To date, surgery is the most preferred treatment, but five year survival rate is often poor. [2, 3]. This is mainly due to the lack of early symptoms in this disease and most of the patients are diagnosed in advanced stages. Generally accepted, human gastric carcinogenesis initiated by normal mucosa, followed by chronic superficial gastritis (CSG), then chronic atrophic gastritis, to intestinal metaplasia, and finally by dysplasia and gastric cancer [4]. Therefore, early prevention on gastric precancerous lesions and diseases could reduce the incidence of GC. In recent decades, diagnostic methods based on endoscopic examination, pathological section and barium meal examination have been widely applied to GC patients [5]. However, these screening methods are limited by various disadvantages, as they are time-consuming, involve a high level of invasiveness, and are laborious and potentially harmful to patients. Thus, establishment of a sensitive, noninvasive examination method for early detection and prognosis prediction in GC patients is of significant importance.

Metabolomics is an emerging science involving the profiling changes in small-molecular metabolites produced by a biological system under certain conditions [6]. It seems to be a very promising method for biomarker discovery due

to the dynamic responses of the metabolome that reflects upstream biological processes in the body. It has several major advantages, such as the readily availability, noninvasive and high sensitivity [7]. For the past few years, metabolomics has been utilized for analysis of metabolic alterations caused by cancers and other diseases, which has led to substantial advances in the discovery of biomarkers and early diagnosis [8]. Ikeda et al. indicated that the changes in the levels of 3-hydroxypropionic acid and pyruvic acid to sufficiently segregate gastric cancer from oesophageal and colorectal cancer and shows high sensitivity and specificity [9]. A recent study demonstrated that a set of amino acid altered in urine sample, including L-alanine, L-isoleucine, L-serine, L-threonine, L-proline and L-methionine, formed a characteristic biosignature for discrimination of GC patients from healthy control population [10].

Biomarkers are small-molecular intermediates and end products of active cellular processes, forming a correlation between molecular metabolic changes and phenotype [11, 12]. Therefore, they reflect alterations of the physiological state of a biological system (cell, tissue or organism) at a certain point in time. There is no doubt that one of the greatest challenges for biomarker-related is discovering biomarkers that accurately distinguish cancer from precancerous stages, where overlapping signs and symptoms (unintentional weight loss or vague epigastric pain) make differential clinical diagnosis difficult [13]. Till now, few studies on metabolic changes for screening and early diagnosis of intestinal-type GC and precancerous stages have been applied in clinical practice, which are needed to be further

explored.

In this work, we developed an ultra-high performance liquid chromatography coupled with quadrupole-time-of-flight mass spectrometry (UPLC-Q-TOF/MS) and metabolomics profiling approach, combined with statistical learning, to validate multiplex biomarker candidates for screening and early diagnosis of GC and precancerous stages (CSG). On the basis of potential biomarkers, the related metabolic pathways and correlation networks were investigated and the global metabolic features were discussed. Furthermore, we used a random forest machine learning approach to diagnose an individual's disease status for each disease based on metabolites abundance. The random forest analysis demonstrates that the differentially metabolites can aid in classifying disease status and may serve in disease diagnosis between chronic superficial gastritis and GC.

Materials and methods

Patient information and sample collection

The present study was approved by the ethics Committee of the People's Hospital of Yangzhong City (Yangzhong, China) and all participants provided written informed consent. A total of 86 individual patients, who had CSG and intestinal-type GC were recruited at the People's Hospital of Yangzhong City between July and December, 2015. Among them, four cases of patients who had a history of chemotherapy or surgical treatment were excluded from this study. All of tissue specimens were examined by gastroscopic biopsy or pathological examination

after surgery. According to the results from pathologic diagnosis, the 82 samples were divided into three groups, including fifty cases of CSG (mean age ± SD, 52.1 ± 7.0 years), seven cases of intestinal-type EGC (mean age ± SD, 66.3 ± 11.9 years) and twenty-five cases of intestinal-type advanced gastric cancer (AGC, mean age ± SD, 67.0 ± 9.7 years). Atrophic gastritis was rare in the real world of Yangzhong City, a well-known high-risk area of gastric cancers in China where our specimens were collected. Thus, we did not enroll cases with atrophic gastritis in the present study [14]. Details of basic information of patients with CSG and intestinal-type GC staging are shown in Table 1. Patient details and clinical pathological information were listed in Table S1. Inclusion criteria are as follows: (a) Adult male or female patients above 18 years old; (b) All participants signed informed consent forms before entering the study; (c) Patients were diagnosed as gastric cancer or chronic superficial gastritis via gastroscopy and biopsy examination. They were newly diagnosed and had not yet receive any treatment, including traditional Chinese medicine, radiotherapy, chemotherapy, surgery or any other therapy.

The exclusion criteria were as follows: Patients with (a) metabolic diseases, such as diabetes, gout or hyperlipidemia; (b) remnant gastric cancer; (c) severe cachexia and expected survival time < 2 months; (d) double or multiple cancers; (e) serious systemic disease of the heart, lung, liver or kidney; (f) serious complications included intestinal paralysis, intestinal obstruction, interstitial pneumonia, pulmonary fibrosis, uncontrolled diabetes, liver and kidney dysfunction; (g) chronic nausea, vomiting or diarrhea (equal to or more than 4 times a day; watery stools); (h)

gastrointestinal haemorrhage and require blood transfusion; (i) human immunodeficiency virus (HIV) or acquired immune deficiency syndrome (AIDS); (j) severe mental illness; (k) grade 2 or higher neuropathy; (l) infectious diseases or inflammation, such as body temperature ≥ 38°C; (m) long-term medications taking known to affect metabolism, such as hormones or immunosuppressive agents; (n) pregnant or breast-feeding.

5 mL venous blood samples from all patients were collected under fasting conditions and added in heparin sodium anti-coagulated tube. The collected whole blood was refrigerated at 4 ℃ within 15 min and centrifuged at 263.84 xg for 15 min within 4 h. Plasma was carefully transferred to an Eppendorf tube, and stored at -80 ℃ until use.

Chemicals and reagents

Acetonitrile, methanol, formic acid and isopropanol were purchased from J. T. Baker Chemical Co. (Phillipsburg, New Jersey, USA). All chemical reagents were HPLC grade. Purified water was produced by a Milli-Q Reagent Water System (Millipore, MA, USA).

Sample preparation

All frozen plasma samples were thawed completely at room temperature. Then, 100 μL plasma samples were transferred to Eppendorf tubes, and 300 μL methanol/acetonitrile solution (v/v, 1:1) containing 2-Chloro-L-phenylalanine (5

μg/mL) as internal standard was added. Mixed sample was vortex-mixed for 30 s and placed at 4 °C for 1 h. Vortex-mix again for 30s and kept at 4°C for 3 h to fully precipitate the protein in the plasma. Finally, the mixture was centrifuged at 14841 xg for 10 min at 4˚C, and the clear supernatant was collected to injection vial for UPLC-Q-TOF/MS analysis.

UPLC-Q-TOF/MS analysis

The metabolomic analysis was carried out on an ACQUITY UPLC (Waters) system equipped with Micromass quadrupole-time-of-flight mass spectrometer (Q-TOF/MS) (Waters Corp., Milford, USA). Plasma metabolites were separated on a Acquity BEH-C18 column (100 mm × 2.1 mm i.d., 1.7 μm; Waters, Milford, USA) with the column oven temperature maintained at 50 °C. Mobile phase A consisted of 0.1% formic acid in water and mobile phase B used the mixture of B-isopropanol, acetonitrile, methanol, formic acid (20: 40: 40: 0.1 (v/v)). The gradient program (A/B, v/v) was changed from 98/2 to 0/100 for 12.5 min with a constant flow rate of 0.4 mL/min. Injection volume was set at 3 μL. MS parameters were as follows: mode, positive ion; capillary voltage, 3000 V; cone voltage, 35 V; collision energy, 3 eV; ion source temperature, 115 °C; desolvent gas temperature, 350 °C; desolvent gas flow, 600 L/h; full scan range, 50-1000 m/z. The mass spectrometric data were recorded with a scan time of 0.3 s and an inter-scan delay of 0.02 s. To evaluate data quality and reliability, a quality control (QC) sample was injected and analyzed once every 10 study samples.

177

178 **Statistical analysis**

179 Orthogonal partial least squares-discriminant analysis (OPLS-DA) was
180 performed by SIMCA-P software (14.0, Umetrics AB), and validated by a
181 permutations test (200 times) [15, 16]. Significantly metabolites between two groups
182 were selected by variable importance in the projection (VIP) > 1 and P < 0.05.
183 According to standard guidelines, metabolites were confirmed by "Level 1"
184 annotations, including at least two orthogonal techniques defining 2D structure, such
185 as MS/MS and RT or CCS [17]. Significantly differential metabolites were identified
186 from the elemental composition and exact mass, from the goodness of the isotopic fit
187 for the predicted molecular formula and from MS/MS fragmentation matching with
188 public databases, including HMDB (https://hmdb.ca/), METLIN
189 (http://metlin.scripps.edu), LIPID MAPS Structure Database (LMSD,
190 http://www.lipidmaps.org/data/structure/), Serum Metabolome
191 (https://serummetabolome.ca/) and Kyoto Encyclopedia of Genes and Genomes
192 (KEGG, https://www.genome.jp/kegg/), using Progenesis QI software (Waters,
193 Milford, MA, USA). MS^2 matching tolerance was set at 0.05 m/z for library
194 matching, with a minimum of three matching ions among MSMS reference and
195 experimental spectra. Metabolic pathway analysis was performed by online
196 MetaboAnalyst 5.0 (https://www.metaboanalyst.ca/). Random Forest model was
197 constructed using scikit-learn (version: 0.23.0), and the parameters were as follows:
198 cv 10, test-size 0.3, random-state 500.

Results

Metabolites detection and identification

A full-scan detection of plasma metabolites was performed by UPLC-Q-TOF/MS, including 50 cases of CSG, 7 cases of intestinal-type EGC and 25 cases of intestinal-type AGC, which involved principal components that account for the majority of the differences in the data. A total of 2203 peaks were detected and 50 differential metabolites were authentically identified, including L-proline, L-isoleucine, L-leucine, L-valine, lysine alanine, lysophosphatidylcholines (LysoPC) (12), phosphatidylcholines (PC) (16), phosphatidylethanolamines (6), L-carnitine, creatine, cholesterol, cholic acid, tyramine, uric acid, capryl carnitine, pyruvaldehyde, docosatrienoic acid, malonaldehyde and 1-sphingosine phosphate.

Differential plasma metabolic profiles among groups

Metabolite differences in CSG and GC

Using SIMCA-P software, the metabolic data were analyzed according to the OPLS−DA model, and the score plot revealed a good separation between CSG and GC patients, as shown in Fig. 1A. R2Y (0.952) and Q2 (0.689) values represented the predictability and goodness of fit, respectively. Statistical validation of corresponding OPLS-DA model was performed by permutation testing (200 iterations) to determine the validity and degree of overfitting. The results showed the Q2 value of -0.317, indicated that OPLS-DA model was not overfitting. According

to the screening criteria of differential metabolites, the differential metabolites were further screened by combining the p value. A total of 8 endogenous metabolites were finally identified as markers and listed in Table 2. Among them, 7 metabolites were found to be up-regulated, whereas 8 to be down-regulated in intestinal-type GC patients compared with CSG patients.

Metabolite differences in CSG and intestinal-type EGC

OPLS-DA as a supervised method was performed to discriminate the overall metabolic profiles between CSG and intestinal-type EGC patients. The score plot of OPLS-DA was presented in Fig. 1B. OPLS-DA (CSG vs EGC) revealed a well gathering trend in score plot. The OPLS-DA model parameters R2Y and Q2 (cum) were 0.963 and 0.639, suggesting good fitness and predictive ability of the OPLS-DA model. A statistical validation of the OPLS-DA model was performed to determine the validity and degree of overfitting with 200 permutation tests. The results showed the Q2 value < 0. Therefore, the OPLS-DA model for discrimination of both of CSG and EGC were successfully established and validated. Six metabolites, named L-carnitine, L-proline, pyruvaldehyde, PC(14:0/18:0), LysoPC(14:0) and lysinoalanine were definited in metabolic profiles. Identification and statistic analysis indicated significant elevation of L-carnitine, L-proline, pyruvaldehyde, PC(14:0/18:0), LysoPC(14:0) and lysinoalanine were definited in metabolic profile, while revealing significant reduction of LysoPC(14:0) and lysinoalanine, in intestinal-type EGC compared with CSG, as shown in Table 3.

Metabolite differences in intestinal-type EGC and AGC

Similarly, a OPLS-DA analysis was used to explore the metabolic profiling differences between the intestinal-type EGC and AGC patients, and the results are presented in Fig. 1C. Score plot of the OPLS-DA revealed a clear segregation of groups. Statistical validation of the OPLS-DA model was performed by permutation analysis. Response permutation tests with 200 permutations showed no overfitting in the models. Based on the criteria of OPLS-DA (VIP > 1 and P < 0.05), 16 statistically differentially expressed metabolic molecules in total were screened out and finally 6 metabolic molecules were identified as potential metabolite biomarkers between the two groups. The significantly changed 6 metabolites listed in Table 4. PC(O-18:0/0:0) and LysoPC(20:4(5Z,8Z,11Z,14Z)) were found to be up-regulated, whereas L-proline, L-valine, adrenic acid and pyruvaldehyde to be down-regulated in intestinal-type AGC patients.

Metabolic Pathway Analysis

On the basis of the detected differential metabolites, pathway analysis was performed by MetaboAnalyst 5.0 to uncover the global metabolic disorders in CSG and intestinal-type GC patients, mainly involved in glycerophospholipid metabolism, primary bile acid biosynthesis, linoleic acid metabolism, valine, leucine and isoleucine biosynthesis, alpha-Linolenic acid metabolism, as shown in Fig. 2A. Fig. 2B presents the major impacted pathways in the CSG-EGC groups, including

lipid-related metabolism, pyruvate metabolism and glycine, serine and threonine metabolism. Analysis of these metabolites which were differentially expressed between EGC and AGC groups, revealed the perturbations of aminoacyl-tRNA biosynthesis, valine, leucine and isoleucine biosynthesis, pantothenate and CoA biosynthesis, ether lipid metabolism and pyruvate metabolism (Fig. 2C). The changes of detected differential metabolites related to the abnormal metabolic pathways, providing clues for underlying the potential metabolic mechanism in intestinal-type GC.

Discriminant models establishment based on the ROC analysis

Each disease state examined in this study has a set of metabolites, prompting the question of whether the differential metabolites can be regarded as identification biomarkers for distinguishing various stages of GC from CSG, used to classify disease status. To answer this question, we constructed random forest models to classify different stages of GC and CSG based on metabolites abundance, and receivers operating characteristic (ROC) curves were used to test the classification. We mainly established three models, namely, CSG vs. GC, CSG vs. EGC, and EGC vs. AGC. The dataset was randomly divided into the training set (70%) and test set (30%) for supervised random forest model calibration and validation, and models were fit using 10-fold cross-validation (500 trees). Result indicated that differential metabolites were able to distinguish GC patients from CSG, with the AUC value 0.79 (Fig. 3A). The model which discriminated between CSG and EGC revealed an

excellent performance with an area under the ROC curve of 1 (Fig. 3B). Among the strongest discriminatory features, Carnitine had the greatest impact, followed by pyruvaldehyde and proline. We found that the model which discriminated between EGC and AGC has moderate ability to predict GC status (AUC = 0.60) (Fig. 3C). This suggests that there may not be enough similarities to classify diseased EGC from AGC. The most likely reason for these results was the small number of sample, and thus affected statistical analyse.

Discussion

In this study, high-throughput metabolomics couple with UPLC-Q-TOF/MS technology was utilized to investigate intestinal-type GC-related metabolic alterations and elucidate potential diagnostic biomarkers. The present evaluation was performed on patients with CSG and two subgroups of intestinal-type GC (EGC and AGC) to search for the correlates between the small molecule metabolites and the disease progression. Most of the metabolites identified were altered on statistically significant level, derived mainly from general biochemical pathways related to amino acid metabolism and lipid metabolism.

Amino acids, as the substrates for protein synthesis, are crucial for cancer cell migration and proliferation. Previous studies have associated amino acid metabolism aberrations with cancer development [18-19]. It is involved in multiple cancers that regulate several signaling pathways, including protein synthesis, cell growth, lipid biogenesis, autophagy and so on [20]. In this study, L-proline was found to be

up-regulated in intestinal-type EGC and AGC stage, and L-valine was also found significantly up-regulated in AGC stage. High levels of proline in tumour tissues cause the overexpression of MMPs which degrades extracellular matrix and degradation of collagen catalysed by proline dehydrogenase, which could promote cell proliferation, energy production and resistance to oxidative stress (act as an antioxidant) [21-25]. L-valine is an essential and important functional amino acid involved in many growth and metabolic processes, and is also a glucogenic amino acid for biosynthesizing macromolecules (e.g., proteins and lipids), which are vital to the growth of cancer cell [26]. The accumulation of amino acids could ascribe to the proliferation by cancer cells, suggesting cancer transformation is linked with adaptive increases in protein synthesis [27]. Except a number of biologic functions, amino acid metabolism is also considered as an essential energy metabolism pathway of cancer cells to meet the high energy requirement [28]. For example, valine could be transformed into pyruvate for energy supply through aerobic glycolysis, resulting in the significant increase in pyruvate [29]. Thus, the up-regulated of valine in intestinal-type GC indicates that cancer cell energy metabolism may be significantly increased during cancer progression

Another important feature in intestinal-type GC progression was the apparent changes of lipids. It is well known that lipids play an important role at cellular and organismal levels, being the dominant structural components of biomembranes and energy storage entities [30]. Additionally, lipids participate in signal transduction and can be broken down into biologically active lipid mediators, which regulate some

carcinogenic processes [31, 32]. In the present study, potential biomarkers analyses revealed significant alterations in plasma LysoPC and PC. The down-regulation of them may be mainly due to the increased demand for membrane constituents during malignant transformation, cancer invasion and metastasis. Dysregulation of choline phospholipid metabolism is associated with carcinogenesis and cancer progression, which has been verified in many biomarker studies [33-35], including studies of GC [36]. Thus, the abnormal levels of LysoPC and PC may be considered as important biomarkers for intestinal-type GC patients.

Glycolysis is a main metabolic mode of cancer cells. Most cancer cells mainly use aerobic glycolysis to generate energy rather than mitochondrial oxidative phosphorylation and produce great numbers of lactate and acidic metabolites, which is known as the “Warburg effect” [37]. Methylglyoxal (also called pyruvaldehyde) is a cytotoxic reactive intermediate of glycolysis [38], whose overexpression was observed in a variety of human cancers [39, 40]. The main metabolic pathway leading to methylglyoxal is related to carbohydrate metabolism and involves enzymatic and nonenzymatic degradation of the triose-phosphate intermediates dihydroxyacetone phosphate and glyceraldehyde 3-phosphate deriving from glycolysis. It should be noted that methylglyoxal can react rapidly with DNA and proteins to produce advanced-glycated end products, and thus promote cell death [41]. The activity of fructose-6-phosphokinase (6-FPK), the enzyme involved in the rate-limiting step of glycolysis, significantly increases in gastric cancer tissues, resulting in low glucose levels [42]. There is cumulative evidence linking the

overexpression of pyruvate kinase with rapid tumour proliferation and poor prognosis, while in vitro studies also suggest that the downregulation of enzymes impair tumour invasion [43].

Furthermore, we evaluated the predictive performance of the metabolites using ROC analyses computed by the random forest algorithm. The model which discriminated between CSG and GC patients had good predictive power, at 0.79 AUC in plasma. The model which discriminated between CSG and EGC revealed an excellent performance with an area under the ROC curve of 1. The AUC for the classification of EGC from AGC was 0.60. The most likely reason for these results was the small number of sample, and thus affected statistical analyse. Overall, the metabolites can aid in classifying disease status and may serve in disease diagnosis. Future studies should consider increasing the sample size, and the inclusion of more clinical variables in the model, which will better evaluate the accuracy of the developed models in early diagnosis.

Conclusion

In this study, UPLC-Q-TOF/MS plasma metabolomics has been successfully applied for biomarker screening in intestinal-type GC. Based on differential metabolites signatures, biomarker panels were defined for the diagnosis of EGC with satisfactory discrimination performance, as well as for AGC. Metabolic pathway analysis indicated that changes in most potential plasma biomarkers were correlated with general biochemical pathways (amino acid metabolism and lipid metabolism),

implying enhanced energy production and cell proliferation. The study highlights the potential advantages of biomarker panels in real clinical diagnostics, which can be used as a promising tool for early-stage intestinal-type GC diagnosis and prognosis.

Abbreviations

AGC: advanced gastric cancer; AUC: area under the curve; CSG: chronic superficial gastritis; EGC: early gastric cancer; GC: Gastric cancer; LysoPC: lysophosphatidylcholine; OPLS-DA: orthogonal partial least squares-discriminant analysis; PC: phosphatidylcholines; PCA: principal component analysis; QC: quality control; ROC: receiver operating characteristic curve; UPLC-Q-TOF/MS: ultra-high performance liquid chromatography coupled with quadrupole-time-of-flight mass spectrometry; VIP: variable importance in the projection.

CRediT authorship contribution statement

Shikai Yan and **Xi Wang** conceived and designed the study. **Xi Wang**, **Shasha Li**, **Jin Li**, **Juming Ma** and **Zhaolai Hua** collected the clinical data and performed the experiments. **Lijing Du** drafted the first version of the manuscript. **Shuai Ji** and **Wenlu Chen** analysed the data. **Shikai Yan**, **Xue Xiao** and **Huizi Jin** revised the manuscript toghther. All authors contributed to the interpretation of the results, edited and approved the final manuscript.

Ethnical approval and consent to participate

According to the Declaration of Helsinki, this study project was evaluated and approved by Institutional Review Board of the 903rd Hospital of PLA (20140501; Hangzhou, China) and Institutional Review Board of People's Hospital of Yangzhong City (IRB201404; Yangzhong, China). Written informed consent was obtained from all participants.

Acknowledgements

This work was supported by the Hangzhou Science and Technology Commission (20140633B41) and the Medical Innovation Project of PLA Nanjing Military Area Command (2013MS150). The Committee of Hangzhou Science and Technology Commission and Medical Innovation Project of PLA Nanjing Military Area Command made a detailed discussion of the scientific validity, reasonableness and feasibility of this study and finally decided to support this study.

References

[1] Bray F, Ferlay J, Soerjomataram I, et al. Global cancer statistics 2018: GLOBOCAN estimates of incidence and mortality worldwide for 36 cancers in 185 countries. CA Cancer J. Clin. 2018; 68(6): 394-424.

[2] D'Angelica M, Gonen M, Brennan MF, et al. Patterns of initial recurrence in completely resected gastric adenocarcinoma. Ann. Surg. 2004; 240: 808-816.

[3] Kamangar F, Dores GM, Anderson WF. Patterns of cancer incidence, mortality, and prevalence across five continents: defining priorities to reduce cancer disparities in different geographic regions of the world. J. Clin. Oncol. 2006; 24: 2137-2150.

[4] Correa P. A human model of gastric carcinogenesis, Cancer Res. 1988; 48: 3554-3560.

[5] Jayavelu ND, Bar NS. Metabolomic studies of human gastric cancer: Review. World J. Gastroenterol. 2014; 20(25): 8092-8101.

[6] Weiss RH, Kim K. Metabolomics in the study of kidney diseases. Nat. Rev. Nephrol. 2011; 8: 22-33.

[7] Wang Z, Liu XY, Liu X, et al. UPLC-MS based urine untargeted metabolomic analyses to differentiate bladder cancer from renal cell carcinoma. BMC Cancer 2019; 19: 1195.

[8] Dettmer K, Aronov PA, Hammock BD. Mass spectrometry-based metabolomics. Mass Spectrom. Rev. 2007; 26: 51-78.

[9] Ikeda A, Nishiumi S, Shinohara M, et al. Serum metabolomics as a novel diagnostic approach for gastrointestinal cancer. Biomed. Chromatogr. 2012; 26(5):

548-558.

[10] Chen Y, Zhang J, Guo L, et al. A characteristic biosignature for discrimination of gastric cancer from healthy population by high throughput GC-MS analysis. Oncotarget 2016; 7(52): 87496-87510.

[11] Tang YQ, Li Z, Lazar L, et al. Metabolomics workflow for lung cancer: Discovery of biomarkers. Clin. Chim. ACTA 2019; 495: 436-445.

[12] Sarma SN, Kimpe LE, Doyon VC. A metabolomics study on effects of polyaromatic compounds in oil sand extracts on the respiratory, hepatic and nervous systems using three human cell lines. Environ. Res. 2019; 178: 108680.

[13] Costello E. A metabolomics-based biomarker signature discriminates pancreatic cancer from chronic pancreatitis. Gut 2018; 67(1): 2-3.

[14] Zheng XZ, Mao XH, Xu K, et al. Massive Endoscopic Screening for Esophageal and Gastric Cancers in a High-Risk Area of China. PLoS One. 2015; 10(12): e0145097.

[15] Kuligowski J, Pérez-Guaita D, Escobar J, et al. Evaluation of the effect of chance correlations on variable selection using Partial Least Squares-Discriminant Analysis. Talanta 2013; 116: 835-840.

[16] Westerhuis JA, Hoefsloot HCJ, Smit S, et al. Assessment of PLSDA cross validation. Metabolomics 2008; 4: 81-89.

[17] Viant MR, Kurland IJ, Jones MR, et al. How close are we to complete annotation of metabolomes? Curr. Opin. Chem. Biol. 2017; 36: 64–69.

[18] Christensen HN. Role of amino acid transport and countertransport in nutrition and metabolism. Physiol. Rev. 1990; 70: 43-77.

[19] Lai HS, Lee JC, Lee PH, et al. Plasma free amino acid profile in cancer patients, Semin. Cancer Biol. 2005; 15: 267-276.

[20] O'Connell TM. The complex role of branched chain amino acids in diabetes and cancer. Metabolites 2013; 3(4): 931-945.

[21] Liu W, Hancock CN, Fischer JW, et al. Proline biosynthesis augments tumor cell growth and aerobic glycolysis: involvement of pyridine nucleotides. Sci. Rep-UK. 2015; 5: 17206.

[22] Elia I, Broekaert D, Christen S, et al. Proline metabolism supports metastasis formation and could be inhibited to selectively target metastasizing cancer cells. Nat. Commun. 2017; 8: 15267.

[23] Sahu N, Cruz DD, Gao M, et al. Proline starvation induces unresolved ER stress and hinders mTORC1-dependent tumorigenesis. Cell Metab. 2016; 24: 753-761.

[24] Szabados L, Arnould S. Proline: a multifunctional amino acid. Trends Plant Sci. 2010; 15: 89-97.

[25] Phang JM, Donald SP, Pandhare J, et al. The metabolism of proline, a stress substrate, modulates carcinogenic pathways. Amino Acids 2008; 35(4): 681-690.

[26] Phang JM. Proline metabolism in cell regulation and cancer biology: recent advances and hypotheses. Antioxid. Redox Sign. 2019; 30(4): 635-649.

[27] Eley HL, Russell ST, Tisdale MJ. Effect of branched-chain amino acids on muscle atrophy in cancer cachexia. Biochem. J. 2007; 407(1): 113-120.

[28] Hong Y, Ho KS, Eu KW, et al. A susceptibility gene set for early onset colorectal cancer that integrates diverse signaling pathways: implication for tumorigenesis. Clin. Cancer Res. 2007; 13: 1107-1114.

[29] Dang CV. Links between metabolism and cancer. Genes Dev. 2012; 26: 877-890.

[30] Chaneton B, Hillmann P, Zheng L, et al. Serine is a natural ligand and allosteric activator of pyruvate kinase M2. Nature 2012; 491: 458-462.

[31] Santos CR, Schulze A. Lipid metabolism in cancer. FEBS J. 2012; 279: 2610-2623.

[32] Perrotti F, Rosa C, Cicalini I, et al. Advances in lipidomics for cancer biomarkers discovery. Int. J. Mol. Sci. 2016; 17: 1992.

[33] Klupczynska A, Plewa S, Kasprzyk M, et al. Serum lipidome screening in patients with stage I non-small cell lung cancer. Clin. Exp. Med. 2019; 19(4): 505-513.

[34] Lu YH, Huang C, Gao L, et al. Identification of serum biomarkers associated with hepatitis B virus-related hepatocellular carcinoma and liver cirrhosis using mass-spectrometry-based metabolomics. Metabolomics 2015; 11: 1526-1538.

[35] Li JN, Xie HY, Li A, et al. Distinct plasma lipids profiles of recurrent ovarian cancer by liquid chromatography-mass spectrometry. Oncotarget 2017; 8(29): 46834-46845.

[36] Cheng ML, Bhujwalla ZM, Glunde K. Targeting Phospholipid Metabolism in Cancer. Front. Oncol. 2016; 6: 266.

[37] Warburg O. On the origin of cancer cells. Science, 1956; 123: 309-314.

[38] Kalapos MP. Methylglyoxal in living organisms: chemistry, biochemistry, toxicology and biological implications. Toxicol. Lett. 1999; 110: 145-175.

[39] Baunacke M, Horn LC, Trettner S, et al. Exploring glyoxalasel expression in prostate cancer tissues: targeting the enzyme by ethyl pyruvate defangs some malignancy-associated properties. Prostat. 2014; 74(1): 48-60.

[40] Fonseca-Sánchez MA., Rodríguez-Cuevas S, Mendoza-Hernández G, et al. Breast cancer proteomics reveals a positive correlation between glyoxalase 1 expression and high tumor grade. Int. J. Oncol. 2012; 41: 670-680.

[41] Desai K, Wu L. Methylglyoxal and advanced glycation endproducts: New therapeutic horizons? Recent Pat. Cardiovasc. Drug Discov. 2007; 2: 89-99.

[42] Gatenby RA, Gillies RJ. Why do cancers have high aerobic glycolysis? Nature Reviews. Cancer 2004; 4(11): 891-899.

[43] Wu J, Hu L, Chen M, et al. Pyruvate kinase M2 overexpression and poor prognosis in solid tumors of digestive system: Evidence from 16 cohort studies. Oncotargets Ther. 2016; 9: 4277–4288.

519 **Legends**

520 **Fig. 1** OPLS-DA score plot among two groups and the results of 200 permutation
521 tests. (A) CSG vs. GC group; (B) CSG vs. EGC group; (C) EGC vs. AGC group.

522 **Fig. 2** Metabolic pathway analysis in intestinal-type GC. (A) CSG vs. GC. 1)
523 Glycerophospholipid metabolism; 2) Primary bile acid biosynthesis; 3) Linoleic acid
524 metabolism; 4) Valine, leucine and isoleucine biosynthesis; 5) Alpha-Linolenic acid
525 metabolism. (B) CSG vs. EGC. 1) Glycerophospholipid metabolism; 2) Linoleic acid
526 metabolism; 3) Alpha-Linolenic acid metabolism; 4) Pyruvate metabolism. (C) EGC
527 vs. AGC. 1) Aminoacyl-tRNA biosynthesis; 2) Valine, leucine and isoleucine
528 biosynthesis; 3) Pantothenate and CoA biosynthesis; 4) Ether lipid metabolism; 5)
529 Pyruvate metabolism.

530 **Fig. 3** ROC curves based on random forest models. (A) CSG vs. GC group; (B) CSG
531 vs. EGC group; (C) EGC vs. AGC group. ROC, receiving operational curve; AUC,
532 area under curve.

533 **Fig.1**

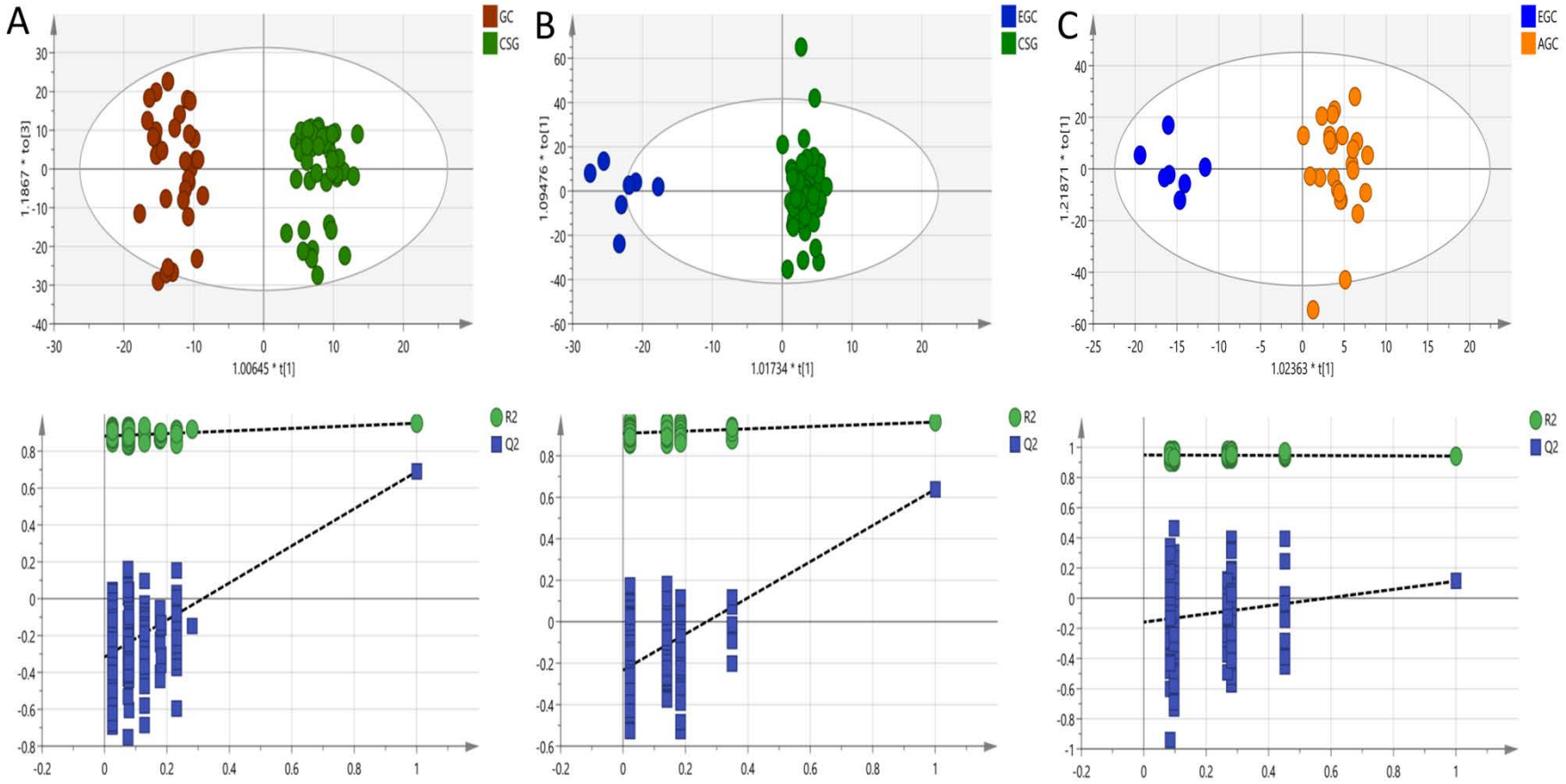

534

535

Fig. 2

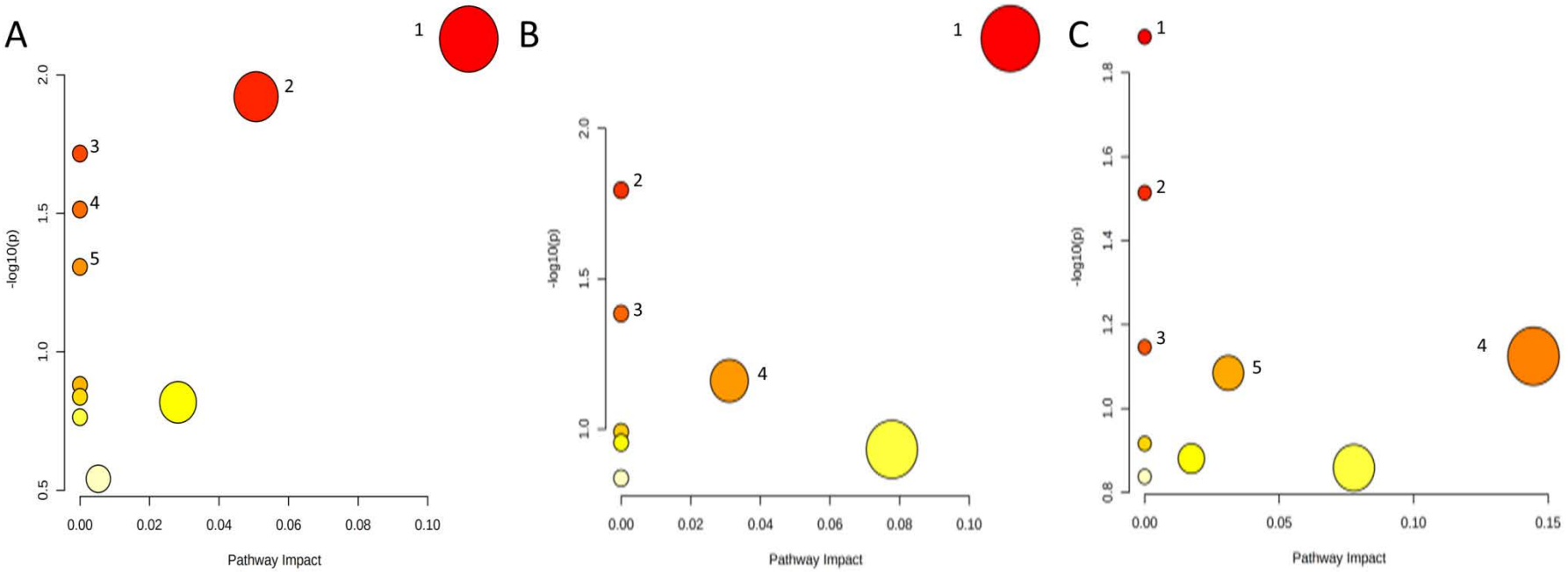

Fig. 3

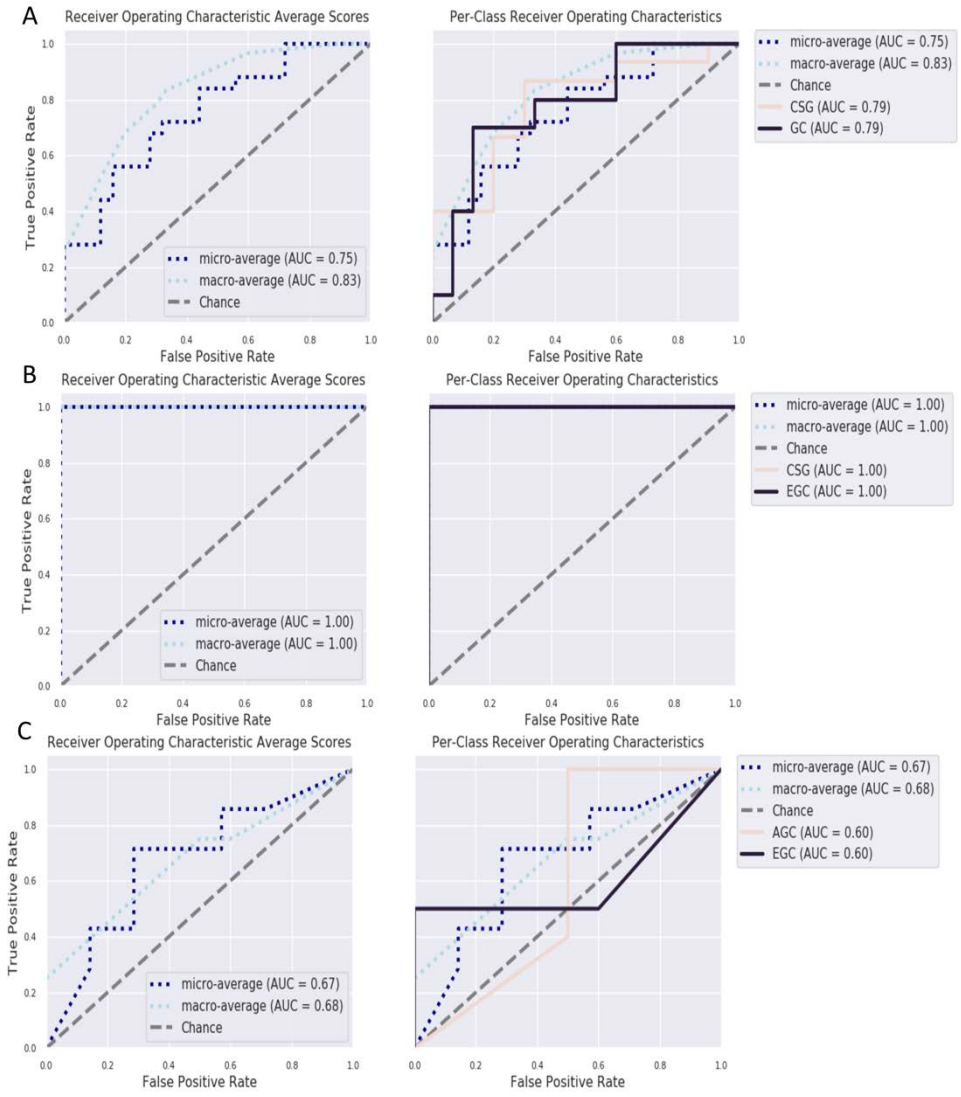
A
Receiver Operating Characteristic Average Scores
True Positive Rate
False Positive Rate
micro-average (AUC = 0.75)
macro-average (AUC = 0.83)
Chance
Per-Class Receiver Operating Characteristics
micro-average (AUC = 0.75)
macro-average (AUC = 0.83)
Chance
CSG (AUC = 0.79)
GC (AUC = 0.79)
B
Receiver Operating Characteristic Average Scores
True Positive Rate
False Positive Rate
micro-average (AUC = 1.00)
macro-average (AUC = 1.00)
Chance
Per-Class Receiver Operating Characteristics
micro-average (AUC = 1.00)
macro-average (AUC = 1.00)
Chance
CSG (AUC = 1.00)
EGC (AUC = 1.00)
C
Receiver Operating Characteristic Average Scores
True Positive Rate
False Positive Rate
micro-average (AUC = 0.67)
macro-average (AUC = 0.68)
Chance
Per-Class Receiver Operating Characteristics
micro-average (AUC = 0.67)
macro-average (AUC = 0.68)
Chance
AGC (AUC = 0.60)
EGC (AUC = 0.60)

Table 1 Demographic and clinical characteristics of study participants.

	CSG	EGC*	AGC*
Gender（Male/ Female）	14/36	6/1	19/6
Age（year）	52.1±7.0	66.3±11.9	67.0±9.7
TNM IA stage	_	7	_
TNM IB stage	_	_	2**
TNM IIB stage	_	_	1
TNM IIIA stage	_	_	9
TNM IIIB stage	_	_	2
TNM IIIC stage	_	_	4
TNM IVstage	_	_	7

*Both EGC and AGC are intestinal-type adenocarcinoma according to Lauren classification. **The TNM stages of two patients classified as IB were both T2N0, which were grouped into AGC.

Table 2 Statistically significant differences in metabolite levels between intestinal-type GC and CSG groups

NO	Compound	Adducts	Retention time(min)	m/z	Formula	Mass Error (ppm)	Level of identification	P value	The trend of GC
1	L-Carnitine	M+H	0.67	162.11	$C_7H_{15}NO_3$	2.91	MS^2	4.43E-06	↑
2	L-Isoleucine	M+H	1.13	132.10	$C_6H_{13}NO_2$	0.96	MS^2	0.00017	↑
3	LysoPC(20:4(8Z,11Z,14Z,17Z))	M+H	5.92	544.34	$C_{28}H_{50}NO_7P$	4.13	MS^2	0.00033	↓
4	LysoPC(18:1(9Z))	M+H	6.64	522.36	$C_{26}H_{52}NO_7P$	7.17	MS^2	0.0082	↓
5	LysoPC(15:0)	M+H	7.63	482.33	$C_{23}H_{48}NO_7P$	2.56	MS^2	0.0057	↓
6	Cholesterol	2M+Na	9.77	795.70	$C_{27}H_{46}O$	2.84	MS^2	0.0054	↑
7	PC(14:0/18:0)	M+H	10.30	734.57	$C_{40}H_{80}NO_8P$	4.55	MS^2	4.96E-05	↑
8	Cholic acid	2M+NH4	10.42	834.61	$C_{24}H_{40}O_5$	3.02	MS^2	0.0022	↓

Table 3 Statistically significant metabolites for comparison of CSG and intestinal-type EGC patients

NO.	Compound	Adducts	Retention time (min)	m/z	Formula	Mass Error (ppm)	Level of identification	P value	The trend of EGC
1	L-Carnitine	M+H	0.67	162.11	$C_7H_{15}NO_3$	2.91	MS^2	0.0081	↑
2	L-Proline	M+Na	2.04	138.06	$C_5H_9NO_2$	24.03	MS^2	0.0003	↑
3	Pyruvaldehyde	M+ACN+H	0.68	114.07	$C_3H_4O_2$	0.54	MS^2	0.0036	↑
4	PC(14:0/18:0)	M+H	10.30	734.57	$C_{40}H_{80}NO_8P$	4.55	MS^2	<0.0001	↑
5	LysoPC(14:0)	M+H	5.65	468.31	$C_{22}H_{46}NO_7P$	1.42	MS^2	0.0081	↓
6	Lysinoalanine	M+NH4	2.85	251.17	$C_9H_{19}N_3O_4$	19.37	MS^2	0.002	↓

Table 4 Statistically significant differences in metabolite levels between intestinal-type EGC and AGC groups

NO	Compound	Adducts	Retention time(min)	m/z	Formula	Mass Error (ppm)	Level of identification	P value	The trend of EGC
1	L-Proline	M+H	2.04	138.06	$C_5H_9NO_2$	1.48	MS^2	0.0113	↓
2	L-Valine	M+H	0.73	118.08	$C_5H_{11}NO_2$	0.32	MS^2	0.0051	↓
3	Adrenic acid	M+Na	4.31	355.26	$C_{22}H_{36}O_2$	11.73	MS^2	0.0159	↓
4	PC(O-18:0/0:0)	M+ACN+H	7.96	551.43	$C_{26}H_{56}NO_6P$	3.95	MS^2	0.0076	↑
5	LysoPC(20:4(5Z, 8Z,11Z,14Z))	M+H	5.91	544.34	$C_{28}H_{50}NO_7P$	4.13	MS^2	0.0153	↑
6	Pyruvaldehyde	M+ACN+H	0.68	114.06	$C_3H_4O_2$	0.54	MS^2	0.0352	↓

573

Table S1 Patient details and clinical pathological information

No.	Type of disease	Age	Sex	TNM stages	Indicator of tumor	Clinical diagnosis	Gastroscopic diagnosis
1	Early gastric cancer	83	male	T1aN0M0 Ⅰ A	CEA: 4.40 ng/mL; CA199: 13.5 U/mL	Gastric adenocarcinoma of the angulus(high differentiation), localized ulcerative type, T1N0M0, old lacunar infarcts	Chronic gastritis, duodenitis, esophagitis, HP-positive
2	Early gastric cancer	72	female	T1aN0M0 Ⅰ A	CEA: 2.70 ng/mL; CA199: 9.23 U/mL	Gastric adenocarcinoma of the angulus (IIc type, T1N0M0)	Flushing and erosion of the gastric angulus
3	Early gastric cancer	72	male	T1aN0M0 Ⅰ A		Adenocarcinoma of the Antrum(Borrmann type II, T1N0M0)	1.5*0.8cm irregular ulcer at the gastric antrum
4	Early gastric cancer	83	male	T1aN0M0 Ⅰ A	CEA: 2.50 ng/mL; CA199: 34.87 U/mL	Gastric adenocarcinoma of the cardia(high differentiation), T1N0M0	Ulcer at the gastric cardia
5	Early gastric cancer	83	male	T1aN0M0 Ⅰ A		Gastric adenocarcinoma of the corpus (high-middle differentiation), presented with superficial bulge, T1N0M0	Malignant tumor to be investigated, chronic gastritis, esophagitis
6	Early gastric cancer	56	male	T1aN0M0 Ⅰ A		Gastric adenocarcinoma of the corpus (low differentiation), signet ring cell carcinoma, ulcerative type, T1N0M0	Chronic gastritis, gastro-duodenal ulcer
7	Early gastric cancer	57	male	T1bN0M0 Ⅰ A	CEA: 8.30 ng/mL; CA199: 23.20 U/mL	Gastric adenocarcinoma of fundus(middle differentiation), ulcerative type, T1N0M0	Malignant Tumor
8	Advanced gastric cancer	84	male	T3N2M0 ⅢA	CEA: 5.50 ng/mL; CA199: 24.80 U/mL	Gastric adenocarcinoma of the corpus (middle differentiation), localized ulcerative type, T3N2M0	Malignant Tumor of the gastric corpus, angulus and antrum
9	Advanced gastric cancer	76	male	T4aN2M O ⅢB	CEA: 1.4 ng/mL; CA199: 23.83 U/mL	Gastric adenocarcinoma of the angulus (middle differentiation, Borrmann II type, T3N2MO)	1.0×1.2 cm ulcer at the gastric antrum

10	Advanced gastric cancer	59	female	T4N1M0 ⅢA	CEA: 5.32 ng/mL; CA199: 60.10 U/mL	Gastric adenocarcinoma of the corpus (middle-low differentiation), ulcerative type, T4N1M0	Malignant tumor at the gastric corpus, angulus and antrum
11	Advanced gastric cancer	72	female	T2N1M1 Ⅳ		Gastric adenocarcinoma at stage IV(peritoneal metastases, low differentiation)	Ulcer of the gastric antrum and angulus, malignant tumor, superficial ulcer of gastro-duodenal, chronic gastritis, inflammatory activity, bile reflux, reflux esophagitis.
12	Advanced gastric cancer	73	female	T2N2M0 ⅡB	CEA: 2.10 ng/mL; CA199: 31.61 U/mL	Gastric adenocarcinoma of the antrum, localized ulcerative type T2N1M0	Ulcer of the gastric corpus and angulus,Malignant Tumor, chronic gastritis, bile reflux
13	Advanced gastric cancer	68	male		CEA: 7.56 ng/mL; CA199: 3.2 U/mL	Gastric malignancies	Chronic superficial gastritis
14	Advanced gastric cancer	86	male	T4aN2M0 ⅢB		Gastric adenocarcinoma of the corpus (middle-low differentiation), infiltrative type, T4N1M0	Irregular ulcer located in the gastric corpus, gastric ulcer, malignant Tumor
15	Advanced gastric cancer	70	male	T2N1M1 Ⅳ	CEA: 262 ng/mL; CA199: 11.30 U/mL	Gastric adenocarcinoma of the angulus	Gastric adenocarcinoma of the angulus
16	Advanced gastric cancer	82	male		CEA: 3.80 ng/mL; CA199: 10.80 U/mL	Gastric adenocarcinoma of the angulus	Ulcer of the gastric antrum and angulus, malignant Tumor
17	Advanced gastric cancer	59	male	T4aN3M0 ⅢC	CEA: 15.10 ng/mL; CA199: 233.71 U/mL	Gastric adenocarcinoma ulcerative type, T3N1M0	Malignant Tumor of the gastric angulus and corpus, chronic gastritis
18	Advanced gastric cancer	74	female	T3N3M1 Ⅳ		Gastric adenocarcinoma of the corpus (low differentiation), ulcerative type,	Gastric malignant tumor, reflux esophagitis.

						T3N2M1	
19	Advanced gastric cancer	81	male	T4aN3M0 ⅢC	CEA: 1.80 ng/mL; CA199: 4.83 U/mL	Gastric adenocarcinoma of the antrum (middle differentiation)with hemorrhage, ulcerative type, T4N2M0	Malignant tumor of the gastric antrum
20	Advanced gastric cancer	72	female	T3N2M0 ⅢA	CEA: 3.50 ng/mL; CA199: 39.78 U/mL	Gastric adenocarcinoma of the angulus (middle differentiation), ulcerative type, T3N2M0	Malignant tumor of the gastric angulus
21	Advanced gastric cancer	67	male	T2N0M0 Ⅰ B	CEA: 6.20 ng/mL; CA199: 29.25 U/mL	Gastric adenocarcinoma of the angulus, IIc type, T1N0M0	Approximately 2.0*2.5 cm flushing and erosions at the gastric angulus, 1.5 cm superficial ulcer
22	Advanced gastric cancer	64	male	T2N0M0 Ⅰ B	CEA: 1.90 ng/mL; CA199: 14.85 U/mL	Gastric adenocarcinoma of the corpus (IIc type, T1N0M0, high differentiation)	Irregular ulcer located in the gastric fundus and lesser curvature
23	Advanced gastric cancer	49	male	T3N2M0 ⅢA		Gastric adenocarcinoma of the antrum (Borrmann type II, T3N2MO, middle differentiation)	Approximately 4.0cm ulcer of the posterior wall of the gastric antrum, irregular uplift in the mucous membrane
24	Advanced gastric cancer	69	male		CEA: 4.25 ng/mL; CA199: 5.10 U/mL; CA50 8.46I U/mL	Gastric malignancies	Gastric ulcer
25	Advanced gastric cancer	57	male	T4N2M1 Ⅳ	CEA: 988.70 ng/mL; CA199: 127.59 U/mL; CA125 733.9 U/mL	Gastric signet ring cell carcinomas, Renal dysfunction	Gastric ulcer
26	Advanced gastric cancer	79	male	T3N2M0 ⅢB		Gastric adenocarcinoma of the corpus (middle-low differentiation), ulcerative	Malignant Tumor

						type, T3N2M0	
27	Advanced gastric cancer	80	female	T3N2M0 IIIA	CEA: 1.70 ng/mL; CA199: 18.77 U/mL	Gastric adenocarcinoma of the antrum (low differentiation) with pyloric insufficiency obstruction, localized ulcerative type, T3N1M0	Malignant Tumor, gastric retention
28	Advanced gastric cancer	83	male	T4aN3M0 IIIC	CEA: 2.50 ng/mL; CA199: 8.72 U/mL	Gastric adenocarcinoma of the antrum, Borrmann type II, T3N3M0	Ulcer at the gastric angulus, swelling
29	Advanced gastric cancer	77	male	T4aN3M O IIIB		Gastric adenocarcinoma of the corpus (middle-low differentiation), ulcerative type, T4N3M0	Malignant tumor at the gastric corpus
30	Advanced gastric cancer	84	male	T4N2MO IIIB	CEA: 4.00 ng/mL; CA199: 19.5 U/mL	Mucinous adenocarcinoma of the antrum, localized infiltrative type, T3N1M0	Erosions were present in the gastric antrum, malignant Tumor, chronic gastritis, mainly of upper part of the stomach
31	Advanced gastric cancer	83	male	T1N0M1 Ⅳ	CEA: 7.29 ng/mL; CA199: 13.83 U/mL; CA50 12.58I U/mL	Gastric malignancies	
32	Advanced gastric cancer	77	male	T3N1M1 Ⅳ		Gastric adenocarcinoma at stage Ⅳ	Malignant Tumor, Chronic superficial gastritis
33	Chronic superficial gastritis	59	female			Chronic gastritis	Antral-predominant gastritis
34	Chronic superficial gastritis	49	male			Chronic gastritis	Antral-predominant gastritis
35	Chronic superficial	59	female			Chronic gastritis	Antral-predominant gastritis

	gastritis				
36	Chronic superficial gastritis	50	female	Chronic gastritis	Antral-predominant gastritis
37	Chronic superficial gastritis	74	male	Chronic gastritis	Antral-predominant gastritis
38	Chronic superficial gastritis	63	male	Chronic gastritis	Antral-predominant gastritis
39	Chronic superficial gastritis	54	female	Chronic gastritis	Chronic gastritis, inflammatory activity, bile reflux(mild)
40	Chronic superficial gastritis	67	female	Chronic gastritis	Chronic gastritis, bile reflux
41	Chronic superficial gastritis	56	female	Chronic gastritis	Antral-predominant gastritis, bile reflux(mild)
42	Chronic superficial gastritis	55	female	Chronic gastritis	Antral-predominant gastritis
43	Chronic superficial gastritis	59	male	Chronic gastritis	Chronic gastritis, erosions were present in the lower part of the gastric antrum
44	Chronic superficial gastritis	53	female	Chronic gastritis	Antral-predominant gastritis
45	Chronic superficial gastritis	55	female	Chronic gastritis	Chronic gastritis, inflammatory activity, erosions were present in the gastric antrum, bile reflux(mild)
46	Chronic superficial gastritis	62	female	Chronic gastritis	Chronic gastritis, polypoid bulge of the gastric corpus
47	Chronic superficial	58	male	Chronic gastritis	Antral-predominant gastritis

	gastritis				
48	Chronic superficial gastritis	63	female	Chronic gastritis	Chronic gastritis, mainly of upper part of the stomach
49	Chronic superficial gastritis	61	female	Chronic gastritis	Antral-predominant gastritis, bile reflux
50	Chronic superficial gastritis	55	male	Chronic gastritis	Antral-predominant gastritis, bile reflux
51	Chronic superficial gastritis	54	female	Chronic gastritis	Antral-predominant gastritis
52	Chronic superficial gastritis	66	female	Chronic gastritis	Chronic gastritis, inflammatory activity, bile reflux
53	Chronic superficial gastritis	50	male	Chronic gastritis	Antral-predominant gastritis
54	Chronic superficial gastritis	60	female	Chronic gastritis	Antral-predominant gastritis
55	Chronic superficial gastritis	47	female	Chronic gastritis	Chronic gastritis, mainly of upper part of the stomach
56	Chronic superficial gastritis	56	male	Chronic gastritis	Chronic gastritis, inflammatory activity, bile reflux
57	Chronic superficial gastritis	50	female	Chronic gastritis	Antral-predominant gastritis
58	Chronic superficial gastritis	52	female	Chronic gastritis	Chronic gastritis, mainly of the the gastric antrum
59	Chronic superficial gastritis	64	female	Chronic gastritis	Chronic gastritis, mainly of upper part of the stomach

60	Chronic superficial gastritis	49	female	Chronic gastritis	Chronic gastritis, mainly of upper part of the stomach, bile reflux
61	Chronic superficial gastritis	57	male	Chronic gastritis	Chronic gastritis, mainly of lower part of the stomach
62	Chronic superficial gastritis	69	female	Chronic gastritis	Antral-predominant gastritis, bile reflux (mild)
63	Chronic superficial gastritis	65	female	Chronic gastritis	Antral-predominant gastritis
64	Chronic superficial gastritis	57	female	Chronic gastritis	Antral-predominant gastritis
65	Chronic superficial gastritis	63	female	Chronic gastritis	Antral-predominant gastritis
66	Chronic superficial gastritis	62	female	Chronic gastritis	Antral-predominant gastritis
67	Chronic superficial gastritis	72	female	Chronic gastritis	Antral-predominant gastritis
68	Chronic superficial gastritis	65	female	Chronic gastritis	Chronic gastritis, erosions were present in the gastric antrum
69	Chronic superficial gastritis	67	male	Chronic gastritis	Antral-predominant gastritis, reflux esophagitis
70	Chronic superficial gastritis	65	female	Chronic gastritis	Antral-predominant gastritis
71	Chronic superficial gastritis	52	female	Chronic gastritis	Antral-predominant gastritis
72	Chronic superficial gastritis	71	female	Chronic gastritis	Chronic gastritis

73	Chronic superficial gastritis	56	male	Chronic gastritis	Chronic gastritis, inflammatory activity, bile reflux
74	Chronic superficial gastritis	57	female	Chronic gastritis	Erosions were present in the gastric antrum, chronic gastritis
75	Chronic superficial gastritis	55	male	Chronic gastritis	Antral-predominant gastritis, bile reflux
76	Chronic superficial gastritis	50	male	Chronic gastritis	Antral-predominant gastritis
77	Chronic superficial gastritis	56	female	Chronic gastritis	Chronic gastritis, inflammatory activity
78	Chronic superficial gastritis	51	female	Chronic gastritis	Antral-predominant gastritis
79	Chronic superficial gastritis	64	male	Chronic gastritis	Antral-predominant gastritis
80	Chronic superficial gastritis	46	female	Chronic gastritis	Antral-predominant gastritis, bile reflux (mild)
81	Chronic superficial gastritis	46	female	Chronic gastritis	Chronic gastritis, mainly of upper part of the stomach, inflammatory activity
82	Chronic superficial gastritis	60	female	Chronic gastritis	Antral-predominant gastritis